Thermopower of Molecular Junctions: An ab Initio Study

San-Huang Ke,*,† Weitao Yang,†,‖ Stefano Curtarolo,‡,§,‖ and Harold U. Baranger§,‖

Department of Chemistry, Department of Mechanical Engineering and Materials Science, Department of Physics, and Center for Theoretical and Mathematical Sciences, Duke University, Durham, North Carolina 27708

ABSTRACT

Molecular nanojunctions may support efficient thermoelectric conversion through enhanced thermopower. Recently, this quantity has been measured for several conjugated molecular nanojunctions with gold electrodes. Considering the wide variety of possible metal/molecule systems—almost none of which have been studied—it seems highly desirable to be able to calculate the thermopower of junctions with reasonable accuracy and high efficiency. To address this task, we demonstrate an effective approach based on the single particle green function (SPGF) method combined with density functional theory (DFT) using B3LYP and PBE0 energy functionals. Systematic good agreement between theory and experiment is obtained; indeed, much better agreement is found here than for comparable calculations of the conductance.

The thermoelectric effect—the direct conversion of heat flow produced by a temperature differential to electric voltage or vice versa[1]—might provide an alternative avenue for meeting future energy needs if its efficacy could be improved.[2] The usual figure of merit is $ZT = S^2 T\sigma/\kappa$ where S, T, σ, and κ are the thermopower (Seebeck coefficient), absolute temperature, and electrical and thermal conductivities, respectively. Increasing ZT beyond 1 is a challenging task because the factors S, σ, and κ are interdependent.[2] In recent years, with the advent of nanotechnology, it was found that in nanostructures, such as thin-film and quantum dot superlattices,[3-5] ZT can increase to about 1. The use of molecular junctions is another recent and promising approach.[6-14] In these devices, the electrodes' Fermi energy can be located very close to the highest occupied or lowest unoccupied molecular orbital (HOMO or LUMO, respectively), thus enhancing the thermopower, and hence ZT, significantly. The thermopower of several molecular junctions with Au electrodes has been measured using scanning tunneling microscopy.[9,10] To search for better thermoelectric systems, it would be useful, considering the vast range of uninvestigated possibilities, to be able to calculate the thermopower of junctions with reasonable accuracy.

In this paper, we calculate the thermopower of nine organic molecules attached to gold leads (see Figures 1 and 2). There is experimental thermopower data[9,10] for six of the molecules investigated: 1,4-benzenedithiol (BDT), 4,4′-dibenzenedithiol (DBDT), 4,4′-tribenzenedithiol (TBDT), 2,5-dimethyl-1,4-
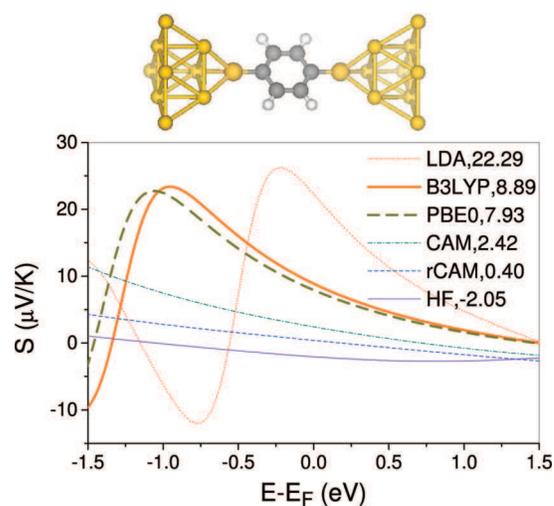

Figure 1. Thermopower calculated for a benzene—dithiol molecular bridge between two Au leads. Different density functionals are used as specified in the legend. The geometry of the bridge plus nine Au atoms on either side is optimized; the remaining Au of the semi-infinite leads is included via the wide band limit approximation. Clearly, the calculated thermopower is strongly affected by the density functional used: LDA leads to a Fermi energy close to the HOMO resonance and a large S; in contrast, HF, CAMB3LYP, and rCAMB3LYP place E_F far from the HOMO resonance and so yield a much smaller S. B3LYP and PBE0 give intermediate results which are in good agreement with experimental values at room temperature.

benzenedithiol (BDT2Me), 2,3,5,6-tetrachloro-1,4-benzene-dithiol (BDT4Cl), and 2,3,5,6-tetraflouro-1,4-benzenedithiol (BDT4F). The other three are similar to TBDT but with four, five, and six benzene rings, denoted by QBDT, PBDT, and HBDT, respectively.

† Department of Chemistry.
‡ Department of Mechanical Engineering and Materials Science.
§ Department of Physics.
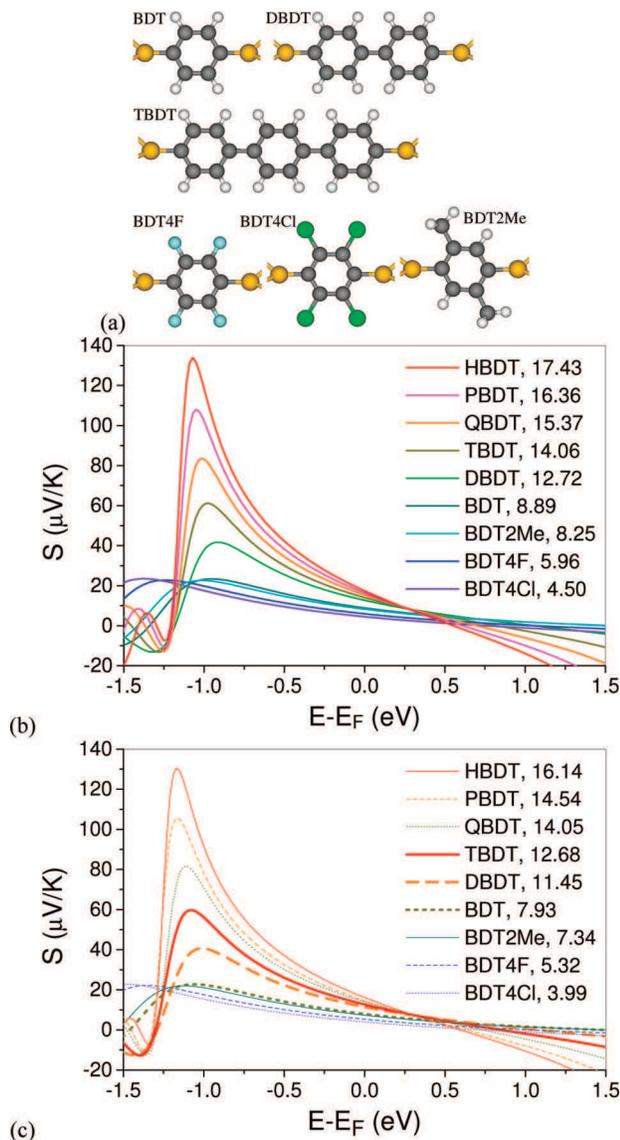‖ Center for Theoretical and Mathematical Sciences.

Figure 2. Thermopower calculated for the molecular junctions shown in (a) using the density functionals of B3LYP (b) and PBE0 (c). The results for the three longer ones (QBDT, PBDT, and HBDT) are also given, whose structures are similar to TBDT but with increasing numbers of benzene ring and are not shown in (a). Color code for the atoms: C, H, Au, F, and Cl are black, gray, yellow, blue, and green, respectively. Note that the longest molecule, HBDT, has the largest thermoelectric effect while the two molecules incorporating electron acceptors (F and CL) have the smallest.

Our theoretical method, combining a Landauer approach to transport based on a single particle green function method (SPGF)[15,16] with ab initio electronic structure methods[17−25] has been described in detail in ref 23.[26] For each molecule, several calculations employing different electronic structure methods were done in order to gauge the dependence of the results on the functional used; comparison with experiment then allows us to choose the optimal functional for these purposes. In particular, we used Hartree−Fock (HF) calculations and density functional theory (DFT) calculations using five different functionals: the local density approximation (LDA), the hybrid functionals B3LYP[27,28] and PBE0,[29] and two very recent orbital-dependent functionals CAMB3LYP[30] and rCAMB3LYP.[31] Previous theoretical work also based

on a SPGF plus DFT treatment[12,14] used only the pure generalized gradient approximation[12] or the LDA[14] and treated the contact structure and electrodes differently.

The system is divided into three parts: left lead, right lead, and device region. The latter contains the molecule plus parts of the leads accommodating the molecule−lead interaction (see Figure 1). The self-consistent HF or DFT Hamiltonian of the device region plus the self-energies of the two semi-infinite leads, $\Sigma_{L,R}(E)$, are used to construct a single-particle Green function, $G_D(E)$, from which the transmission coefficient is calculated as a function of energy: $\tau(E) = Tr[\Gamma_L G_D \Gamma_R G_D^{\dagger}]$, where $\Gamma_{L,R}(E) = i[\Sigma_{L,R}(E) - \Sigma_{L,R}^{\dagger}(E)]$ is the coupling to the left or right lead. Finally, the thermopower is calculated[6]

$$S = -\frac{1}{3e}\pi^2 k_B^2 T \frac{\partial \ln \tau(E)}{\partial E}\bigg|_{E=E_F} \quad (1)$$

where e is the charge of a proton, k_B is the Boltzmann constant, and T is the average temperature of the junction (300 K here). In this paper, S refers to either the value at the Fermi energy, $E = E_F$, when we give a number (as in the Table) or a function of E (in the Figures).

The gold electrodes (leads) are modeled with two gold clusters in the [111] direction with the anchoring S atoms located at the hollow sites (see Figure 1). To improve the efficiency of the computation, mostly spent dealing with the self-energies of the two semi-infinite leads $\Sigma_{L,R}(E)$, we make use of a wide-band limit (WBL) approximation: $\Gamma(E) = -\gamma I$ with $\gamma = 2.5$ eV and I the identity matrix. The molecule−lead coupling is included explicitly in the Hamiltonian because 18 Au atoms are contained in the central device region. Since the density of states of bulk gold is quite flat around E_F, the use of the WBL for the Au atoms in the semi-infinite leads is reasonable, as discussed later. For all the systems, the atomic positions of the molecular bridge, including the molecule−lead separation, are geometrically optimized by minimizing the atomic forces until they are smaller than 0.05 eV/Å. The Fermi energy for our finite cluster is determined by introducing a small smearing (0.027 eV) and using the Fermi function.

Figure 1 shows results for the Au−BDT−Au system. The form of the density functional clearly has a large effect on the result. A key difference is the placement of the Fermi energy with respect to the HOMO resonance: LDA places it very close causing S to be large, while HF, CAMB3LYP, and rCAMB3LYP place it much further away, leading to a much smaller S. B3LYP and PBE0 give similar, intermediate results, 8.89 μV/K (B3LYP) and 7.93 μV/K (PBE0). These values are in good agreement with the experimental data, 8.7 ± 2.1 μV/K[9] and 7.2 ± 0.3 μV/K[10] at room temperature, suggesting that these two functionals are reasonably accurate for calculating thermopower.

Since they were successful for BDT, we only consider B3LYP and PBE0 in treating the other molecular junctions. The results are shown in Figure 2 and compared with experiment in Table 1. It is found that the position of E_F in the B3LYP calculation is slightly closer to the HOMO resonance than in PBE0. As a result, the B3LYP results for S are systematically larger than those from PBE0 by a small

Table 1. Calculated and Experimental Thermopower for the Six Molecular Junctions Shown in Figure 2[a]

	BDT	DBDT	TBDT	QBDT	PBDT	HBDT
B3LYP	8.89	12.72	14.06	15.37	16.36	17.43
PBE0	7.93	11.45	12.68	14.05	14.54	16.14
expt	8.7 ± 2.1^b	12.9 ± 2.2^b	14.2 ± 3.2^b			
	7.2 ± 0.3^c					

	BDT4F	BDT4Cl	BDT2Me
B3LYP	5.96	4.50	8.25
PBE0	5.32	3.99	7.34
expt	5.4 ± 0.4^c	4.0 ± 0.6^c	8.3 ± 0.3^c

[a] Also listed are the calculated values for the three longer molecular bridges (QBDT, PBDT, and HBDT). Results for two density functionals are given; reassuringly, they differ by only about 12%. Note that the calculated values are in remarkably good agreement with the experiment for the six molecules. [b] Experimental values from ref 9. [c] Experimental values from ref 10.
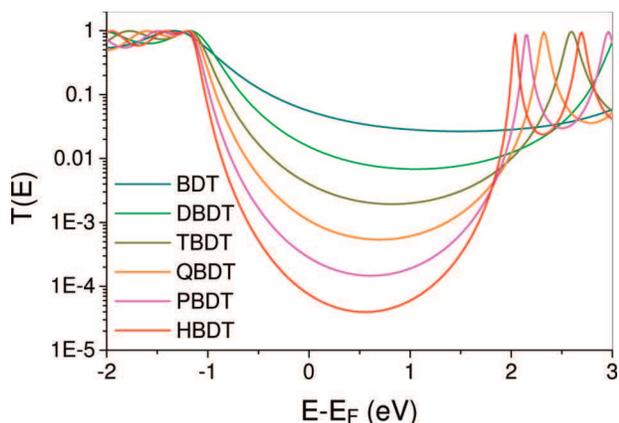
Figure 3. Transmission as a function of energy through the six molecular bridges, BDT, DBDT, TBDT, QBDT, PBDT, and HBDT, given by the B3LYP calculation. The transmission at the Fermi energy (0 here) decreases exponentially, leading to an increased thermopower.

amount, about 12%. The first conclusion from Table 1 is that the calculated and experimental values are in very good agreement, almost within error bars in all cases. Such agreement is in striking contrast to the disagreement typically found for the conductance in such molecular bridges.

There are several trends evident from the data, both theoretical and experimental, in Table 1. First, for increasing length of the bridging molecule, from BDT to HBDT, S increases monotonically. This can be understood[12] by looking at the behavior of ln $\tau(E)$, shown in Figure 3 (B3LYP calculation). Notice that the position and height of the HOMO resonance are approximately fixed. Further, the transmission at E_F, which is in the gap, decreases exponentially as a carbon ring is added, presumably because the tunneling distance increases. Thus the slope of ln $\tau(E)$ increases, and so S increases.

The second trend is that, upon substituting electronegative end groups into BDT (fluorine or chlorine), S becomes substantially smaller. This is an electron-withdrawing effect: the electron withdrawing shifts the E_F away from the HOMO resonance (see Figure 2), reducing S. Thus we find $S_{BDT4F} > S_{BDT4Cl} > S_{BDT}$, as in the experiment.[10] There is a subtle situation for the BDT2Me junction: Our calculation yields an S similar to that of BDT because the electron-withdrawing or donating effect of methyl groups is small (see Figure 2);

however, the experiment[10] found a slightly larger value of S which was ascribed to electron donating. Although the overall agreement between theory and experiment is very good, further work is needed to clarify the order of S_{BDT} and S_{BDT2Me}.

The two trends provide a clue to improving thermoelectric properties of molecular junctions. Although the increasing molecular length enhances considerably S, the exponentially decay of conductance will lead to an overall decreasing contribution to ZT. This can be overcome by shifting the Fermi energy closer to HOMO (or LUMO) resonance, which can be achieved by (1) chemical modification of the moelcule (i.e., electron withdrawing or donating), (2) changing the workfunction of the lead surfaces, and (3) applying a gate (doping).

The effect of molecular vibrations and resulting inelastic scattering is not included in the calculations reported here. As discussed previously by others,[12] the experimental S as a function of molecular length exhibits rather good linearity,[9] suggesting that vibrations are not playing an important role and therefore that the thermopower is dominated by coherent electron transport. Indeed, for such short molecules and hence nearly ballistic transport, this behavior is expected.

Since the WBL approximation is used here, we would like to check its applicability and the sensitivity of our results to its parameter γ. Previously, in applying this approximation to metallic carbon nanotubes,[32] we found that it is very successful for energies around E_F where the density of states is a constant: $\tau(E)$ obtained by using first-principles self-energies in that energy window can be nearly reproduced. Here we would like to check it again. In Figure 4a we show the electronic density of states (DOS) for bulk gold (calculated by DFT-LDA using a four-atom cell and 13500 Monkhorst k points). This DOS is very flat over a wide energy range around E_F. Because we are primarily concerned with the behavior at E_F, the use of the WBL approximation for the Au−Au interaction is therefore reasonable. To determine γ, we find the value that reproduces the overall shape of the transmission coefficient $\tau(E)$ given by full first-principles self-energies. We obtain $\gamma = 2.5$ eV for the present Au(111) leads ($\gamma = 3.0$ eV was used previously for Au(001) leads).[33] Panels b and c show $\tau(E)$ and $S(E)$ for the TBDT junction (B3LYP calculation), respectively, for different γ (2.0, 2.5, and 3.0 eV). Neither $\tau(E)$ nor $S(E)$ is very sensitive to the value of γ. The variation of S is minor and still within the experimental error bar.[9]

We close with some comments on the very good agreement here between theory and experiment. It is well-known that the SPGF-DFT method usually overestimates the equilibrium conductance of conjugated molecular junctions.[34−37] For example, the conductance of a Au−BDT−Au junction given by the present B3LYP and PBE0 calculations is 0.055 and 0.050G_0, respectively ($G_0 = 2e^2/h$ is the conductance quantum). These values are considerably larger than a measured result,[38] ∼0.011G_0. Possible reasons include differences between the experimental and theoretical geometry or deficiencies in the theoretical treatment[39] such as the self-interaction error.[40,41] The latter leads to overly extended charge distributions and thus to an overestimate of the broadening of the HOMO and
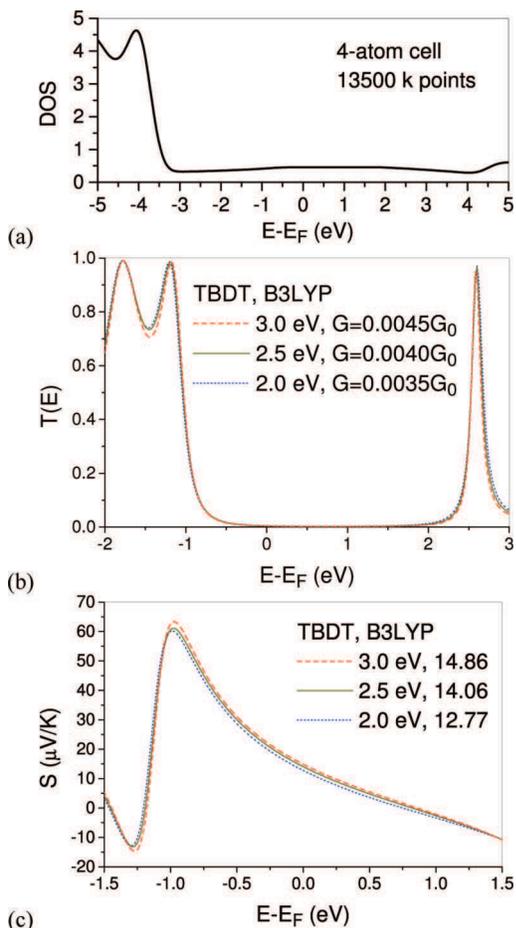
Figure 4. Effect of the parameter γ in the WBL approximation. (a) Density of states (DOS) of bulk gold, calculated by DFT-LDA. (b) Conductance and (c) thermopower of the Au−TBDT−Au junction using different γ values as indicated in the legend. The variation of S is minor and still within the experimental error bar.

LUMO states. While the conductance is very sensitive to this broadening, the thermopower may be much less sensitive: because it is the logarithmic derivative of $\tau(E)$ (see eq 1), d ln $\tau(E)/\mathrm{d}E = (1/\tau)(\mathrm{d}\tau/\mathrm{d}E)$, factors affecting d$\tau$ may cancel those in τ. Sensitivity is supressed as long as the sum of the HOMO and LUMO widths is smaller than the energy gap from E_F to the HOMO or LUMO resonance.[6,10] This condition is met for the systems we have calculated: from Figure 2, $(E_{LUMO} - E_F) > (E_F - E_{HOMO}) \geq 1$ eV while the HOMO and LUMO widths are about $0.1-0.4$ eV. The thermopower, then, is a quantity which is intrinsically less sensitive to some of the problems in the SPGF-DFT method, allowing for a more accurate theoretical estimate.

In summary, we have presented ab initio calculations for the thermopower of various molecular junctions (SPGF-DFT-WBL approach with gold electrodes). The use of the WBL approximation makes the computation very efficient. Systematic good agreement is obtained between theoretical and experimental results by using the B3LYP and PBE0 functionals. The approach demonstrated here is a good candidate for future high-throughput calculations of thermoelectricity in molecular junctions.

References

(1) Ashcroft, N. W.; Mermin, N. D. *Solid State Physics*; Holt, Rinehart, and Winston: New York, 1976.
(2) Majumdar, A. *Science* **2004**, *303*, 777–778.
(3) Venkatasubramanian, R.; Siivola, E.; Colpitts, T.; O'Quinn, B. *Nature* **2001**, *413*, 597–602.
(4) Harman, T. C.; Taylor, P. J.; Walsh, M. P.; LaForge, B. E. *Science* **2002**, *297*, 2229–2232.
(5) Hsu, K. F.; et al. *Science* **2004**, *303*, 818–821.
(6) Paulsson, M.; Datta, S. *Phys. Rev. B* **2003**, *67*, 241403.
(7) Koch, J.; von Oppen, F.; Oreg, Y.; Sela, E. *Phys. Rev. B* **2004**, *70*, 195107.
(8) Segal, D. *Phys. Rev. B* **2005**, *72*, 165426.
(9) Reddy, P.; Jang, S.-Y.; Segalman, R. A.; Majumdar, A. *Science* **2007**, *315*, 1568–1571.
(10) Baheti, K.; Malen, J. A.; Doak, P.; Reddy, P.; Jang, S.-Y.; Tilley, T. D.; Majumdar, A.; Segalman, R. A. *Nano Lett.* **2008**, *8*, 715–719.
(11) Kubala, B.; König, J.; Pekola, J. *Phys. Rev. Lett.* **2008**, *100*, 066801.
(12) Pauly, F.; Viljas, J. K.; Cuevas, J. C. *Phys. Rev. B* **2008**, *78*, 035315.
(13) Murphy, P.; Mukerjee, S.; Moore, J. *Phys. Rev. B* **2008**, *78*, 161406.
(14) Finch, C. M.; García-Suárez, V. M.; Lambert, C. J. *Phys. Rev. B* **2009**, *79*, 033405.
(15) Haug, H.; Jauho, A.-P. *Quantum Kinetics in Transport and Optics of Semiconductors*; Springer-Verlag: Berlin, 1996.
(16) Datta, S. *Electronic Transport in Mesoscopic Systems*; Cambridge University Press: Cambridge, England, 1995.
(17) DiVentra, M.; Pantelides, S. T.; Lang, N. D. *Phys. Rev. Lett.* **2000**, *84*, 979–982.
(18) Taylor, J.; Guo, H.; Wang, J. *Phys. Rev. B* **2001**, *63*, 245407.
(19) Damle, P. S.; Ghosh, A. W.; Datta, S. *Phys. Rev. B* **2001**, *64*, 201403(R).
(20) Xue, Y.; Datta, S.; Ratner, M. A. *Chem. Phys.* **2002**, *281*, 151–170.
(21) Brandbyge, M.; Mozos, J.-L.; Ordejón, P.; Taylor, J.; Stokbro, K. *Phys. Rev. B* **2002**, *65*, 165401.
(22) Louis, E.; Vergés, J. A.; Palacios, J. J.; Pérez-Jiménez, A. J.; SanFabián, E. *Phys. Rev. B* **2003**, *67*, 155321 (5 pages).
(23) Ke, S.-H.; Baranger, H. U.; Yang, W. *Phys. Rev. B* **2004**, *70*, 085410.
(24) Rocha, A. R.; Garcia-Suarez, V.; Bailey, S. W.; Lambert, C. J.; Ferrer, J.; Sanvito, S. *Phys. Rev. B* **2006**, *73*, 085414.
(25) Arnold, A.; Weigend, F.; Evers, F. *J. Chem. Phys.* **2007**, *126*, 174101.
(26) In the present work, the wave functions are expanded using a Gaussian 6-311G** basis set for C, H, and S atoms, and a CRENBS basis set for Au atoms.[42]
(27) Becke, A. D. *J. Chem. Phys.* **1993**, *98*, 5648.
(28) Lee, C.; Yang, W.; Parr, R. G. *Phys. Rev. B* **1988**, *37*, 785.
(29) Adamo, C.; Barone, V. *J. Chem. Phys.* **1999**, *110*, 6158.
(30) Yanai, T.; Tew, D. P.; Handy, N. C. *Chem. Phys. Lett.* **2004**, *393*, 51–57.
(31) Cohen, A. J.; Mori-Sanchez, P.; Yang, W. *J. Chem. Phys.* **2007**, *126*, 191109.
(32) Bulat, F. A.; Ke, S.-H.; Yang, W.; Couchman, L. *Phys. Rev. B* **2008**, *77*, 153401.
(33) Ke, S.-H.; Yang, W.; Baranger, H. U. *Nano Lett.* **2008**, *8*, 3257–3261.
(34) Xue, Y.; Datta, S.; Ratner, M. A. *J. Chem. Phys.* **2001**, *115*, 4292–4299.
(35) Xue, Y.; Ratner, M. A. *Phys. Rev. B* **2003**, *68*, 115407–115418.
(36) DiVentra, M.; Lang, N. D.; Pantelides, S. T. *Chem. Phys.* **2002**, *281*, 189.
(37) Ke, S.-H.; Baranger, H. U.; Yang, W. *J. Chem. Phys.* **2007**, *127*, 144107.
(38) Xiao, X.; Xu, B.; Tao, N. J. *Nano Lett.* **2004**, *4*, 267–271.
(39) Koentopp, M.; Chang, C.; Burke, K.; Car, R. *J. Phys.: Condens. Matter* **2008**, *20*, 083203.
(40) Toher, C.; Filippetti, A.; Sanvito, S.; Burke, K. *Phys. Rev. Lett.* **2005**, *95*, 146402.
(41) Ke, S.-H.; Baranger, H. U.; Yang, W. *J. Chem. Phys.* **2007**, *126*, 201102.
(42) NWChem, A Computational Chemistry Package for Parallel Computers, Pacific Northwest National Lab, Richland, WA, 2003.

NL8031229